Atmospheric Environment 246 (2021) 118175

Contents lists available at ScienceDirect

Atmospheric Environment

journal homepage: http://www.elsevier.com/locate/atmosenv

Isotope signatures of atmospheric mercury emitted from residential coal combustion

Xinyu Li [a,b,1], Zhonggen Li [a,c,*,1], Ji Chen [d,a], Leiming Zhang [e], Runsheng Yin [f], Guangyi Sun [a], Bo Meng [a], Zikang Cui [a,b], Xinbin Feng [a,b,**]

[a] State Key Laboratory of Environmental Geochemistry, Institute of Geochemistry, Chinese Academy of Sciences, Guiyang, 550081, China
[b] University of Chinese Academy of Sciences, Beijing, 100049, China
[c] School of Resources and Environment, Zunyi Normal College, Zunyi, 563006, China
[d] College of Chemical Engineering, Huaqiao University, Xiamen, 361021, China
[e] Air Quality Research Division, Science and Technology Branch, Environment and Climate Change Canada, Toronto, M3H 5T4, Canada
[f] State Key Laboratory of Ore Deposit Geochemistry, Institute of Geochemistry, Chinese Academy of Sciences, Guiyang, 550081, China

HIGHLIGHTS

- Isotope signature of total Hg is consistent between flue gas and feed coal
- Obvious MDF occurred among different Hg species in the flue gas
- Significant MIF is observed for Hg^{2+} due to the oxidation of Hg^0
- RCC is an important Hg source and potentially impacts atmospheric Hg isotope composition

GRAPHICAL ABSTRACT

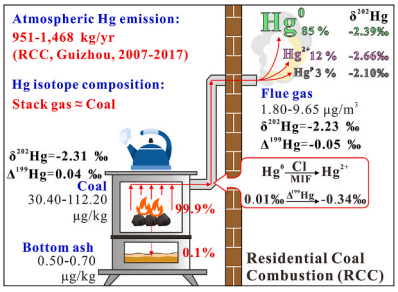

ARTICLE INFO

Keywords:
Atmospheric emissions
Residential stove
Mercury isotopes
Isotope fractionation
Geochemical tracer

ABSTRACT

Residential coal combustion (RCC) is a major source of atmospheric mercury (Hg) in rural areas of China, but little is known about the isotope signatures of Hg from this source. In the present study, the isotope compositions of speciated Hg (Hg^0, Hg^{2+}, and Hg^p) in flue gas emitted from RCC were investigated in two important coal-producing areas (Xingren (XR) and Jinsha (JS)) of Guizhou Province, Southwest China. The total Hg concentration in discharged flue gas is in the range of 1.80–9.65 μg/m^3 at the two sites, and the emission ratio reaches 99.87%. Isotope signatures of total Hg in flue gas are similar to those of Hg in feed coal, with near-zero Δ^{199}Hg and negative δ^{202}Hg (−1.47‰ for XR and −3.00‰ for JS) in discharged flue gas. Such isotope signatures are very different from those of Hg emissions from modern coal-fired power plants with much higher δ^{202}Hg signals. Negative shifts from Hg^0 to Hg^{2+} in flue gas for δ^{202}Hg (−0.94‰) and Δ^{199}Hg (−0.51‰) were observed, suggesting that both mass-dependent fractionation and mass-independent fractionation occurred during RCC. The nuclear volume effect produced by chlorine oxidation of Hg^0 to Hg^{2+} may play an important role in the observed

* Corresponding author. State Key Laboratory of Environmental Geochemistry, Institute of Geochemistry, Chinese Academy of Sciences, Guiyang, 550081, China.
** Corresponding author. State Key Laboratory of Environmental Geochemistry, Institute of Geochemistry, Chinese Academy of Sciences, Guiyang, 550081, China.
E-mail addresses: lizhonggen@mail.gyig.ac.cn (Z. Li), Fengxinbin@mail.gyig.ac.cn (X. Feng).
[1] These authors contributed equally to this work.

https://doi.org/10.1016/j.atmosenv.2020.118175
Received 14 June 2020; Received in revised form 24 December 2020; Accepted 27 December 2020
Available online 31 December 2020

mass-independent fractionation in Hg^{2+}. Without any air pollution control devices, RCC potentially increases the atmospheric Hg levels and has a negative-shifting impact on the $\delta^{202}Hg$ of atmospheric Hg.

1. Introduction

Mercury (Hg) is a pollutant of global concern due to its capability of long-range migration in the atmosphere and bioaccumulation in the food chain. Atmospheric Hg emissions can come from anthropogenic sources (e.g., fossil fuel combustion, nonferrous metal smelting, cement production, waste incineration) and natural sources (e.g., volcanic eruption, forest fires, re-emission of previously deposited Hg from terrestrial and marine ecosystems) (Driscoll et al., 2013; Wang et al., 2018). Anthropogenic Hg emissions have significantly increased since global industrialization and have caused adverse effects on the ecological environment and human health (Streets et al., 2011; Tian et al., 2010; Adlane et al., 2020).

China has been regarded as the largest anthropogenic Hg emitter in the world for the past several decades (AMAP/UNEP, 2008; Streets et al., 2005; Wu et al., 2016), although the total amount of Hg emissions has been substantially reduced from 825 tons/yr in 2005 to 444 tons/yr in 2017 (AMAP/UNEP, 2008; Liu et al., 2019) by adopting modern emission control technologies, e.g., the upgraded air pollution control devices (APCDs), in the major source sectors of coal-fired power plants (CFPPs), coal-fired industrial boilers (CFIBs), and nonferrous smelting (Li et al., 2019a; Liu et al., 2019; Tong et al., 2020; Wu et al., 2016). Coal combustion is one of the largest anthropogenic Hg emission sources in China (Wang et al., 2000; Streets et al., 2005; Zhang et al., 2015). Hg retention efficiency from large and medium scale coal combustion facilities (e.g., CFPPs and CFIBs) has been improved by the installation rate of modern APCDs to over 90% (Li et al., 2019b; Tong et al., 2020), resulting in the total emissions from CFPPs in China declining by more than a half during the past 10 years, e.g., from 105 tons in 2007 to 48 tons in 2017 (Zhang et al., 2015; Liu et al., 2019). However, some small and uncontrolled coal burning facilities, such as residential coal combustion (RCC), have extremely high Hg emission ratios (95.52–99.81%) and consume relatively stable amounts of coal over the years (Cui et al., 2019; Li et al., 2019c). As a result, their relative contributions to the national total Hg emissions are increasing despite consuming much less coal than large facilities (Wu et al., 2016). Coal consumption by RCC in China reached 9.28×10^7 tons in 2017 (National Bureau of Statistic of China, 2019), from which the atmospheric Hg emissions were estimated to be 19–38 tons/yr (Zhang et al., 2015; Zhao et al., 2015). Meanwhile, Hg emissions from coal combustion in China are largely unevenly distributed geographically, with Inner Mongolia, Ningxia, Shanxi, Guizhou, and Hebei Provinces having the greatest per capita Hg emissions (Gao et al., 2019). Four out of these five provinces possessing large coal reserves are located in north China, and one (Guizhou) is located in Southwest China. The cold and damp conditions in the Yunnan-Guizhou Plateau and the abundant coal resources warrant the coal as an essential energy source for residents in Guizhou, especially in rural areas.

Unfortunately, RCC using coal with high contents of harmful elements (e.g., fluorine and arsenic) for heating and cooking resulted in prevalent endemic disease (e.g., dental and skeletal fluorosis and hyperkeratosis) in some areas in Guizhou before the 2000s (Zheng et al., 1999; Finkelman and Centeno, 2020). A recent estimation showed that the annual emission of Hg from RCC in this province doubles the amount from CFPPs (Cui et al., 2019), making it one of the leading emission sources in this province (Liu et al., 2019). In addition, the atmospheric Hg concentration was obviously higher in the heating period than in the non-heating period in Guizhou (Feng et al., 2003; Fu et al., 2011; Fu and Feng, 2015), indicating the nonnegligible contribution of RCC to local and regional atmospheric Hg pollution. However, knowledge of detailed atmospheric Hg emissions and the corresponding isotope signatures of RCC is still limited.

Hg isotope signatures of different emission sources are useful tools in tracking emission sources and investigating the geochemical cycling of Hg (Blum et al., 2014; Kwon et al., 2020; Sonke, 2011). Seven natural stable isotopes of Hg (Hg^{196}, Hg^{198}, Hg^{199}, Hg^{200}, Hg^{201}, Hg^{202}, and Hg^{204}) undergo mass dependent fractionation (MDF) and mass independent fractionation (MIF) during Hg biogeochemical cycling in the environment. The Hg isotope composition for worldwide coal has been summarized by Sun et al. (2016a), including the impacts of location, forming period, rank, and other parameters on the Hg isotope composition of coal. However, significant isotope fractionation of Hg would occur during coal combustion processes involving Hg volatilization, oxidation, and adsorption; thus, significant differences in Hg isotope signatures between atmospheric emissions and feed coal (Sun et al., 2014), or between different Hg species, e.g., gaseous elemental mercury (Hg^0), gaseous oxidized mercury (Hg^{2+}) and particulate mercury (Hg^p), in flue gas were observed (Tang et al., 2017). Therefore, more studies are needed to investigate the Hg isotope signatures of atmospheric emissions and isotope fractionation between speciated Hg in different burners to track the Hg emission sources.

In the present study, coal, bottom ash and speciated Hg (Hg^0, Hg^{2+}, and Hg^p) in flue gas were systematically sampled in residential stoves from two important coal-producing areas in Guizhou Province, Southwest China, and were analyzed for Hg contents and isotope compositions. The objectives of this study are to (1) evaluate atmospheric Hg emissions from RCC; (2) understand Hg isotope fractionation during RCC; and (3) estimate the Hg isotope fingerprints of Hg from RCC.

2. Methodology

2.1. Study area and sampling

Guizhou Province in Southwest China is one of the largest coal-producing areas in China (Fig. 1a and b) (Annals of Coal Industry of Guizhou Province, 1989; Dai and Finkelman, 2017), and had a coal output of 1.63×10^8 tons in 2017 (National Bureau of Statistic of China, 2019). Lump anthracite (Fig. 1c) is commonly combusted in residential stoves (Fig. 1d) for heating and cooking in counties and rural regions in cold winter and wet rainy seasons. The general residential stove in these study areas is cylindrical, with space below the combustion chamber for accommodating bottom ash and fire pan above the chamber for cooking (Fig. 1d and e). The chimney of the residential stove is on the side of the fire pan and leads flue gas out of the room (Fig. 1f).

In the winter of 2018, residential coal, bottom ash, and different Hg species in flue gas (Hg^0, Hg^{2+}, and Hg^p) were collected from local residential stoves in two areas, Xingren County (XR) and Jinsha County (JS), where are important coal producing areas in Guizhou. Coal collected from these two areas was formed in the Late Permian (Fig. 1a and b). The XR coalfield covers areas of 10,000 km^2, with a predicted reserve of 6.8×10^9 tons. The JS coalfield is affiliated with the Zunyi coalfield, which has a coal-bearing area of 7,500 km^2 and a predicted reserve of 1.6×10^{10} tons. In addition, the coals selected in this study are anthracite with low ash and sulfur contents, which are mainly provided for civil and industrial use (Annals of China Coal-Volume of Guizhou Province, 1994; Annals of Coal Industry of Guizhou Province, 1989). The method for flue gas collection is the Ontario Hydro Method (OHM, ASTM Method 6784–02, 2008), which sampled the flue gas outside the room from the chimney of residential stove and separated Hg in the flue gas into three operationally defined Hg species (Fig. S1), i.e., Hg^0, Hg^{2+}, and Hg^p. The details of OHM are described in the Supporting Information (SI).

Our previous study showed that most Hg in coal evaporates in the

first hour (Li et al., 2019c). Flue gas sampling started immediately after ca. two kilograms of lump coal were added into the stove, and lasted until the feed coal was almost burned out, for a period of approximately 2.5–3.0 h. The Hg concentration obtained in the flue gas represents the mean value of the flue gas from this batch of coal, and then a new batch of feed coal was added for another round of sampling. The feed coal and bottom ash were collected from each sampling run before and after sampling, respectively. The feed lump coal was 3–10 cm in diameter, and a portion of each piece of coal to be burned was knocked down to make a composite sample and to reduce the possible sampling bias. Two sets of samples were collected in each household of XR and JS, including solid samples (coal and bottom ash) and flue gas samples (filters for Hg^p, and trapping solutions for Hg^{2+} and Hg^0). In addition, the concentrations of SO_2, NO_x, and CO and the temperature in the flue gas were also measured 30 min after adding coal to the residential stove with a Testo 350 portable flue gas analyzer (Germany, Fig. 1f).

2.2. Hg concentration and isotope composition analysis

Air-dried solid samples were first homogenized and ground into sizes smaller than 150 μm in diameter before being analyzed for Hg contents. Cold vapor atomic absorption spectrophotometry (CVAAS, Lumex RA915+, Russia) was adopted to determine the total Hg contents, which heated solid samples at 800 °C and measured the released Hg^0. The instrument has a detection limit of 0.1 μg/kg. The Hg content in each solid sample was measured at least three times to obtain a mean value. The pretreatment of OHM absorption fluid for total Hg analysis is as follows: 5% *w/v* $KMnO_4$ is added into the KCl and H_2O_2 + HNO_3 impingers until an enduring purple color appears, while 10% *w/v* $NH_2OH{\cdot}HCl$ solution is added into the $H_2SO_4 + KMnO_4$ impingers until a pink or slight purple color is obtained. The Hg concentration in each capture solution was measured by another type of CVAAS (F732S, Shanghai Huaguang Instrument Corp.) after the reduction of Hg^{2+} to Hg^0 by $SnCl_2$, which had a detection limit of 0.05 μg/L.

Solid samples were pretreated by a double-stage tube furnace for Hg isotope analysis as described in detail in SI (Sun et al., 2013). Hg concentrations in the trapping solutions for solid samples and OHM absorption fluids for flue gas samples were diluted to 1 ng/mL in 10% acid before isotope analysis by multiple-collector inductively coupled plasma mass spectrometry (MC-ICP-MS, Nu Plasma II, U.K.), following a previously reported method (Yin et al., 2010). NIST 3133 Hg standard solutions were prepared, with Hg concentration and acid matrices matching the sample solutions. MDF and MIF are reported as $\delta^{xxx}Hg$ and $\Delta^{xxx}Hg$ values (SI), following the convention suggested by Blum and Bergquist (2007).

2.3. Quality assurance and quality control

Materials used for flue gas sampling were carefully precleaned before fieldwork to reduce the system blank and possible contamination. Quartz fiber filters for collecting Hg^p were heated for 2 h at 500 °C. All sampling lines (quartz glass and Teflon tubings), borosilicate glass impingers and bottles were soaked into 20% HNO_3 overnight in the laboratory and washed with deionized water. The systematic blank of ambient air sampling was determined in the laboratory before each field experiment and was found to be < 0.03 μg/m^3 for the total Hg concentration. All vessels used in laboratory analysis were also soaked into 20% HNO_3 and washed with deionized water. HNO_3 and HCl used for treating samples or analysis were double-distilled to remove possible impurities. The Hg concentrations of the systematic and reagent blanks were below the detection limits of CVAAS and MC-ICP-MS in the concentration and isotope analyses, respectively.

For the proximate analysis that includes the moisture content, ash yield, and volatile matter, certified reference materials (CRMs, ZBM095 for anthracite and ZBM113 for bituminous coal) were measured and yielded a deviation of <7% from the certified values for ash yield, and volatile matter. CRMs of NIST SRM 1632d (coal) and NIST SRM 1633c (coal fly ash) were also measured along other solid samples for Hg content, which yielded a deviation of <10% from the certified values. To ensure no Hg isotope fractionation during pretreatment of solid samples (double-stage furnace trapping), the recoveries of total Hg of samples and CRMs (NIST SRM 1632d) were calculated, which ranged from 88% to 95%. In addition, CRMs (UM-Almadén and NIST SRM 1632d) were analyzed and yielded isotope compositions consistent with previously published data (Table S1) (Blum and Bergquist, 2007; Estrade et al., 2010; Sun et al., 2013, 2014).

2.4. Calculation of the Hg emission parameter and isotope mass balance

The emission ratio (ER, %), emission factor (EF, mg Hg/ton coal) and atmospheric emission (AE) of Hg from RCC were calculated according to Eqs. (1)–(3):

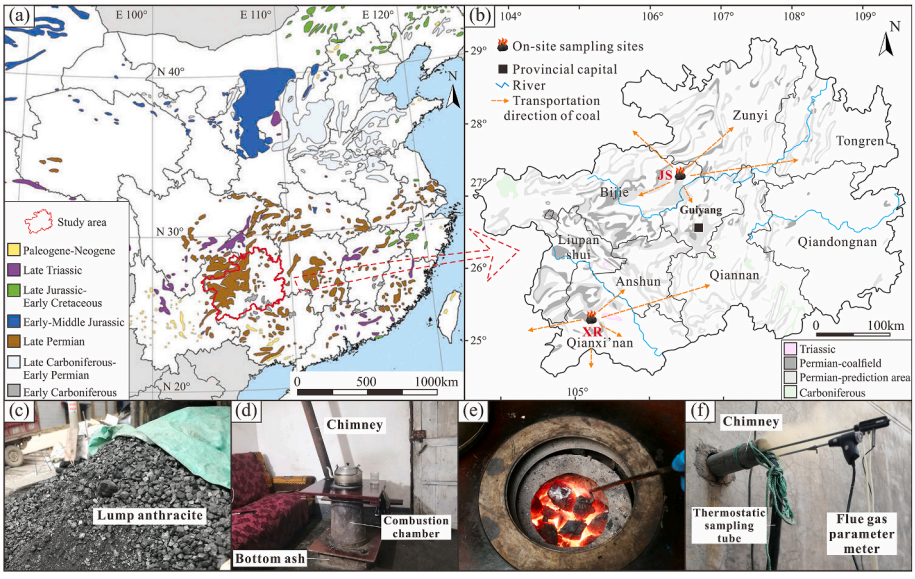

Fig. 1. Distribution and formation ages of coal in China (a, modified from Dai and Finkelman, 2017) and Guizhou Province (b, modified from Annals of Coal Industry of Guizhou Province, 1989), schematic diagram of sampling sites (b), and on-site sampling photos (c, d, e, f).

$$ER = 1 - \frac{C_{Ash}^{Hg} \times A_{ad}}{C_{Coal}^{Hg}} \quad (1)$$

$$EF = C_{Coal}^{Hg} \times ER \quad (2)$$

$$AE = EF \times MC_{Coal} \quad (3)$$

where C_{Ash}^{Hg} and C_{Coal}^{Hg} are the Hg content (μg/kg) in bottom ash and feed coal, respectively; A_{ad} is ash yield (%) of coal with the subscript "ad" representing air-dried basis; and MC_{Coal} is residential coal consumption (ton) for Guizhou Province.

The isotope composition of total Hg in flue gas ($\delta^{202}Hg^T$, $\Delta^{199}Hg^T$) can be calculated based on the three speciated Hg in flue gas as expressed in Eqs. (4) and (5):

$$\delta^{202}Hg_{Flue\ gas}^{T} = \frac{\delta^{202}Hg^{p} \times C_{Flue\ gas}^{p} + \delta^{202}Hg^{2+} \times C_{Flue\ gas}^{2+} + \delta^{202}Hg^{0} \times C_{Flue\ gas}^{0}}{C_{Flue\ gas}^{p} + C_{Flue\ gas}^{2+} + C_{Flue\ gas}^{0}} \quad (4)$$

$$\Delta^{199}Hg_{Flue\ gas}^{T} = \frac{\Delta^{199}Hg^{p} \times C_{Flue\ gas}^{p} + \Delta^{199}Hg^{2+} \times C_{Flue\ gas}^{2+} + \Delta^{199}Hg^{0} \times C_{Flue\ gas}^{0}}{C_{Flue\ gas}^{p} + C_{Flue\ gas}^{2+} + C_{Flue\ gas}^{0}} \quad (5)$$

where $\delta^{202}Hg^T$, $\delta^{202}Hg^p$, $\delta^{202}Hg^{2+}$, and $\delta^{202}Hg^0$ are the $\delta^{202}Hg$ values of total Hg, Hg^p, Hg^{2+}, and Hg^0 in flue gas emitted from RCC, respectively; $\Delta^{199}Hg^T$, $\Delta^{199}Hg^p$, $\Delta^{199}Hg^{2+}$, and $\Delta^{199}Hg^0$ are $\Delta^{199}Hg$ values for total Hg, Hg^p, Hg^{2+}, and Hg^0 in flue gas emitted from RCC, respectively; and $C_{Flue\ gas}^{p}$, $C_{Flue\ gas}^{2+}$, and $C_{Flue\ gas}^{0}$ are Hg concentrations (μg/m^3) of Hg^p, Hg^{2+}, and Hg^0 in flue gas from RCC, respectively.

The combustion process during RCC is not as complicated as that of modern CFPPs which are installed with different APCDs for NOx, SO_2, and PM (particulate matter) controls (Li et al., 2019a; Wu et al., 2016), and most of the Hg in residential coal enters into the flue gas and is discharged into the ambient air by venting pipes (Cui et al., 2019). Hence, the Hg isotope mass balance can be evaluated by calculating the Hg isotope composition of the feed coal and flue gas using Eqs. (6)–(9):

$$\delta^{202}Hg_{Coal}^{A} = \frac{\sum_0^i \delta^{202}Hg_{Coal} \times C_{Coal} \times M_{Coal}}{\sum_0^i C_{Coal} \times M_{Coal}} \ (i = 1, 2, 3\ldots) \quad (6)$$

$$\Delta^{199}Hg_{Coal}^{A} = \frac{\sum_0^i \Delta^{199}Hg_{Coal} \times C_{Coal} \times M_{Coal}}{\sum_0^i C_{Coal} \times M_{Coal}} \ (i = 1, 2, 3\ldots) \quad (7)$$

$$\delta^{202}Hg_{Flue\ gas}^{A} = \frac{\sum_0^j \delta^{202}Hg_{Flue\ gas}^{T} \times C_{Flue\ gas}^{T} \times V_{Flue\ gas}}{\sum_0^j C_{Flue\ gas}^{T} \times V_{Flue\ gas}} \ (j = 1, 2,\ \ 3\ldots) \quad (8)$$

$$\Delta^{199}Hg_{Flue\ gas}^{A} = \frac{\sum_0^j \Delta^{199}Hg_{Flue\ gas}^{T} \times C_{Flue\ gas}^{T} \times V_{Flue\ gas}}{\sum_0^j C_{Flue\ gas}^{T} \times V_{Flue\ gas}} \ (j = 1, 2,\ \ 3\ldots) \quad (9)$$

where $\delta^{202}Hg_{Coal}$ and $\Delta^{199}Hg_{Coal}$ are values of feed coal for RCC; C_{Coal} and M_{Coal} are Hg concentration (μg/kg) in feed coal and coal consumption (kg) for the corresponding test, respectively; $C_{Flue\ gas}^{T}$ and $V_{Flue\ gas}$ are the Hg concentration (μg/m^3) in flue gas and sampling volume (m^3) of flue gas, respectively; A and T in the superscript stand for the weighted average and total Hg, respectively; and i and j represent the number of tests.

2.5. Statistics and data processing

In this study, the mean values of different groups were compared with one-way analysis variance (ANOVA) and independent-samples T tests in SPSS 21.0, where differences were significant at $p < 0.05$. Origin 2017 and CorelDRAW 2018 were used to draw the figures.

3. Results and discussion

3.1. Fuel properties

The proximate analysis of coal in this study is shown in Table 1. Coal samples from both XR and JS are classified into extra low ash coal (ash yields < 10%) according to the Chinese national standard for coal quality of ash (GB 15224.1–2018) based on their ash yield of 6.88% and 7.21%, respectively. The moisture in coal samples is very low (1.61–2.49%), but the concentration of volatiles in coal from JS (13.28 ± 1.99%) is higher ($p < 0.05$) than that from XR (7.58 ± 0.99%). The ash yield in residential coal of this study is significantly lower ($p < 0.01$) than that of coal from CFPPs in Guizhou (30.7–45.7%) (Li et al., 2019b; Tang et al., 2016), and the heat value of residential coal in these two areas (28–30 MJ/kg) (Cui et al., 2019) is also higher ($p < 0.01$) than that used in CFPPs (17–20 MJ/kg) in Guizhou (Li et al., 2019b; Tang et al., 2016), indicating that the quality of feed coal used for RCC is better relative to that used for CFPPs in Guizhou Province.

3.2. Hg in solid and flue gas samples

The Hg content of solid samples (coal and bottom ash) and speciated Hg concentration in the flue gas are illustrated in Table 2 and Fig. 2. Coal samples from XR (112.20 ± 10.60 μg/kg) have significantly higher Hg contents than those from JS (30.40 ± 3.00 μg/kg), but the Hg contents in their bottom ash are comparable (0.70 versus 0.50 μg/kg). The Hg content in XR coal is comparable with previously reported values at Xingren Coalfield (142 ± 43 μg/kg, N = 5, Dai et al., 2005), and worldwide average Hg content (100 ± 10 μg/kg, Ketris and Yudovich, 2009; Yudovich and Ketris, 2005), while the Hg content in JS coal is significantly lower than that of the average value in Guizhou Province (155 μg/kg, N = 108, weighted mean, Li et al., 2013) and the mean value of China (163 μg/kg, N = 1,666, Dai et al., 2012). The ER of Hg calculated using Eq. (1) is 99.95% and 99.78% for residential coal in XR and JS, respectively, which is similar to a previously reported value (99.63%) in Guizhou in 2011–2012 (Cui et al., 2019), indicating that most of the Hg in coal is volatilized into ambient air during residential combustion. Without APCDs installed with residential stoves, most Hg is emitted into the atmosphere from the chimney with flue gas, and a small portion of Hg may also be released into indoor air and impose direct exposure to humans living in the room (Li et al., 2019c; Zhang et al., 2019).

The total Hg concentration in the flue gas of coal from XR is 9.65 ± 0.22 μg/m^3, of which 95.97% is in the form of Hg^0 (9.26 ± 0.27 μg/m^3), and 3.54% is in the form of Hg^{2+} (Table 2). Much lower concentrations are found from the flue gas of JS coal (1.80 ± 0.71 μg/m^3), and Hg^0 and Hg^{2+} account for 74.63% and 20.44%, respectively. Hg^p concentrations are small (<0.10 μg/m^3) in the flue gas of both XR and JS (Table 2), which may be related to the low ash yield in coals (6.88–7.21%, Table 1). Total Hg in flue gas was found to be closely related to Hg content in feed coal (Cui et al., 2019). In addition, the combustion status in residential coal burning is very different from that in boilers of CFPPs, with vigorous combustion for the latter involving pulverized coal and injected air but tender combustion for the former with lump coal burning. Thus, in the case of burning the same amount of coal and similar coal quality, RCC products less PM into flue gas than industrial boilers (Fig. 1e). In addition, the short venting time of flue gas through

Table 1
Proximate analysis of different fuels.

Region	Coal type	Proximate analysis (%, Mean±1σ, N = 2)		
		M_{ad}	V_{ad}	A_{ad}
XR	Lump anthracite	1.61 ± 0.03	7.58 ± 0.99	6.88 ± 0.65
JS	Lump anthracite	2.49 ± 0.03	13.28 ± 1.99	7.21 ± 0.44

Note: M, moisture; V, volatile; A, ash; Subscript "ad", air-dried basis.

Table 2
Hg concentration and proportion in solid samples and flue gas of the RCC.

Samples	Hg content	Proportion (%)		Hg content	Proportion (%)	
	XR (Mean±1σ, N = 2)	Flue gas	Input/ Output[a]	JS (Mean±1σ, N = 2)	Flue gas	Input/ Output[a]
Coal (μg/kg)	112.20 ± 10.60	–	100.00	30.40 ± 3.00	–	100.00
Bottom ash (μg/kg)	0.70 ± 0.00	–	0.05	0.50 ± 0.00	–	0.22
Flue gas Hg^p (μg/m^3)	0.05 ± 0.01	0.49	0.49	0.09 ± 0.03	4.93	4.92
Flue gas Hg^{2+} (μg/m^3)	0.34 ± 0.04	3.54	3.53	0.37 ± 0.25	20.44	20.40
Flue gas Hg^0 (μg/m^3)	9.26 ± 0.27	95.97	95.93	1.35 ± 0.33	74.63	74.46

[a] , Based on the proportion of speciated Hg in flue gas.

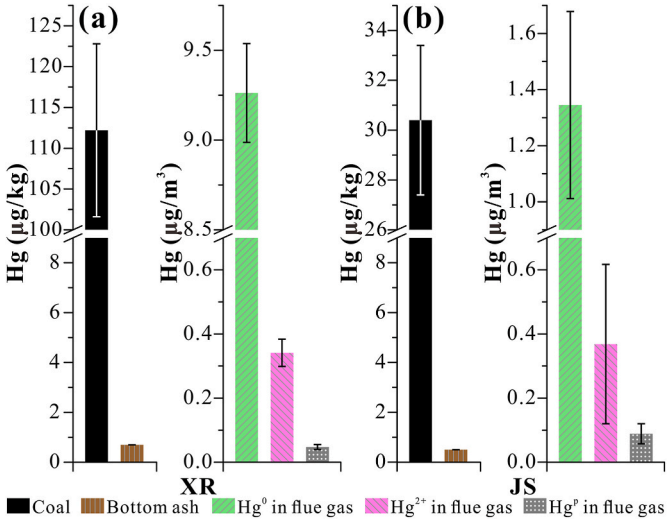

Fig. 2. Hg content in solid samples and speciated Hg in flue gas from RCC in XR (a) and JS (b).

residential vent pipes is not conducive for Hg^p formation. Although the total Hg concentration is much different between XR and JS, their Hg^{2+} concentrations are comparable (0.34 μg/m^3 versus 0.37 μg/m^3). This phenomenon may be related to the limited oxidizing substance (e.g., chlorine, oxygen or metal oxides) in flue gas (Zhang et al., 2016; Zhou et al., 2015). A previous study indicated that Hg^0 accounts for 83.0–96.1% of the total Hg emissions from RCC in Guizhou (Cui et al., 2019), which is comparable to the proportion of Hg^0 in this study (95.97% for XR and 74.63% for JS). However, more Hg^0 (>70%) is oxidized in the flue gas duct of CFPPs before entering wet flue gas desulfurization due to oxidation by catalysts of selective catalytic reduction for NOx and other oxidants in flue gas or PM (Yang and Pan, 2007; Zhang et al., 2016). As a result, a lesser portion of Hg^0 was discharged from CFPPs in Guizhou (average 63.29%, N = 14), achieving a high Hg removal efficiency (average 95.7%) after the combination of APCDs for NOx, PM, and SO_2 (Guizhou Environmental Monitoring Center Station and Institute of Geochemistry, 2016; Li et al., 2019b).

3.3. Hg isotope composition in feed coal and flue gas

Hg isotopes of bottom ash were not analyzed because of the low Hg concentration (0.50–0.70 μg/kg). The Hg isotopes of coal and flue gas samples in this study showed negative $\delta^{202}Hg$ values (Fig. 3a, Table 3). Most residential coal in Guizhou Province is anthracite formed in the Late Permian (Fig. 1b and c), and the Hg isotope composition in coal is controlled by terrestrial plants and crustal rocks (Sun et al., 2016a). The $\delta^{202}Hg$ of coal from XR is −1.59 ± 0.23‰, similar to previously reported values in Guizhou (−1.27 ± 0.65‰, N = 14) (Biswas et al., 2008; Sun et al., 2014; Yin et al., 2014). The $\delta^{202}Hg$ value in XR coal (−1.59 ± 0.23‰) might be related to hydrothermal alteration (~0‰) during the coal forming process (Lefticariu et al., 2011). The $\delta^{202}Hg$ of coal from JS is −2.99 ± 0.85‰, which is much lower than previously reported values in this area (Biswas et al., 2008; Sun et al., 2016a; Yin et al., 2014) and is probably inherited from the original nature of plants (−3.16‰ to −2.43‰ for $\delta^{202}Hg$) in the coal-forming areas in Southwest China (Wang et al., 2020a). A recent study showed that Late Permian coals in eastern Yunnan Province neighboring to western Guizhou also have notable negative $\delta^{202}Hg$ signals (−3.43‰ to −4.34‰) and low Hg contents (8–58 ng/g) (Zheng et al., 2020), which are similar to the coals of JS in this study.

Near zero $\Delta^{199}Hg$ was observed for coals from XR (−0.05 ± 0.01‰) and JS (0.12 ± 0.03‰) (Fig. 3b), which is similar to the average value of Guizhou coal ($\Delta^{199}Hg$ = 0.03 ± 0.09‰, N = 14, 1σ) reported previously (Biswas et al., 2008; Sun et al., 2014; Yin et al., 2014). The high oxygen content (up to 30%) in atmospheric environment in the Late Permian induced more wild fires than during the other periods (Scott and Glasspool, 2006), and the fire-related organic Hg loss in swamps increased the $\Delta^{199}Hg$ value of the resulting coals (Sun et al., 2016a), which have a circum-zero $\Delta^{199}Hg$, which is ~0.2‰ higher than the $\Delta^{199}Hg$ of coals formed during the other periods (Sun et al., 2014, 2016a). In addition, the hydrothermal alteration of coal would also result in a positive $\Delta^{199}Hg$ than that not having been alternated (Sun et al., 2016a; Zheng et al., 2018). However, the insignificant difference between the $\Delta^{199}Hg$ value of this study (−0.05‰–0.12‰) and other ranks of coal in Guizhou or other parts of the world (Sun et al., 2014, Fig. 4a) might be due to the small sample numbers or small wild fire/-hydrothermal alteration effect in the study areas.

After combustion, the majority of Hg in feed coal was volatilized into the flue gas (Table 3), resulting in $\delta^{202}Hg$ variation in different speciated Hg. For speciated Hg in flue gas in XR, Hg^0 ($\delta^{202}Hg$ = −1.38 ± 0.25‰) is isotopically heavier than Hg^{2+} ($\delta^{202}Hg$ = −2.32 ± 0.27‰) and Hg^p ($\delta^{202}Hg$ = −2.77 ± 0.24‰), but the difference is insignificant between Hg^{2+} and Hg^p. However, there is no significant difference in $\delta^{202}Hg$ between Hg^0 (−2.82 ± 0.39‰), Hg^{2+} (−3.01 ± 0.36‰), and Hg^p (−2.94 ± 0.33‰) in flue gas in JS. The $\Delta^{199}Hg$ values of Hg^p and Hg^0 fluctuate around zero, with range of −0.13‰–0.11‰ at these two sites. $\Delta^{199}Hg$ values for Hg^{2+} in flue gas are −0.28 ± 0.01‰ and −0.40 ± 0.08‰ in XR and JS, respectively (Fig. 3, Table 3), which are significantly different ($p < 0.01$) from Hg^p and Hg^0 in flue gas and coals in this study. The possible mechanisms are discussed in Section 3.5 below.

3.4. Hg isotope mass balance

The high emission ratio (99.78–99.95%) of Hg in the residential stove indicates that almost all Hg in coal enters the flue gas during combustion. Thus, the Hg isotope mass balance is evaluated by comparing Hg isotopes in coal and flue gas. Based on Eqs. (6)–(9) and the data in Table 3, the weighted average Hg isotope composition of coal and total Hg in flue gas are illustrated in Fig. S2. Taking $\delta^{202}Hg$ as an example, the weighted average $\delta^{202}Hg$ of coal from XR (−1.55‰) and JS (−3.07‰) are statistically identical to those of their corresponding flue gas (−1.47‰ for XR and −3.00‰ for JS) (Table S2). The disparity of the weighted average $\Delta^{199}Hg$ between coal and total flue gas is 0.05‰–0.14‰, which is statistically insignificantly different considering that

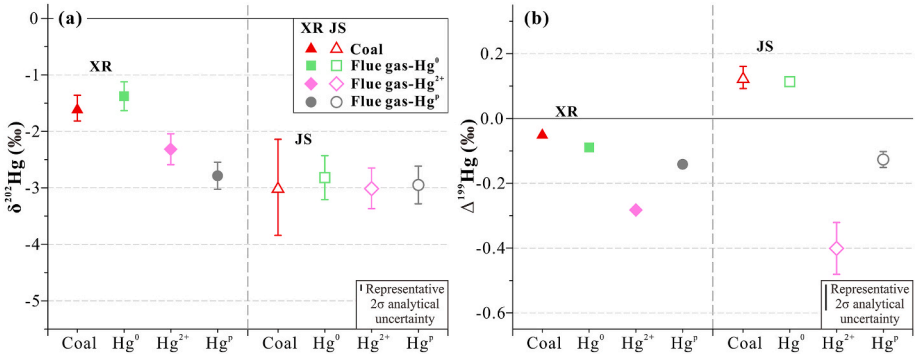

Fig. 3. Hg isotope composition of δ^{202}Hg (a) and Δ^{199}Hg (b) in coal and flue gas from the RCC.

Table 3
Hg isotope composition (‰) in solid samples and flue gas of the RCC.

Region	Samples	δ^{199}Hg	1σ	δ^{200}Hg	1σ	δ^{201}Hg	1σ	δ^{202}Hg	1σ	Δ^{199}Hg	1σ	Δ^{200}Hg	1σ	Δ^{201}Hg	1σ
XR	Coal	−0.45	0.05	−0.76	0.09	−1.20	0.16	−1.59	0.23	−0.05	0.01	0.04	0.03	−0.01	0.02
(N = 2)	Bottom ash	–	–	–	–	–	–	–	–	–	–	–	–	–	–
	Flue gas Hg^0	−0.44	0.05	−0.68	0.14	−1.00	0.15	−1.38	0.25	−0.09	0.01	0.02	0.01	0.04	0.04
	Flue gas Hg^{2+}	−0.87	0.08	−1.11	0.14	−1.88	0.21	−2.32	0.27	−0.28	0.01	0.05	0.00	−0.14	0.00
	Flue gas Hg^P	−0.82	0.08	−1.38	0.14	−2.15	0.18	−2.77	0.24	−0.12	0.02	0.02	0.03	−0.06	0.01
JS	Coal	−0.63	0.18	−1.42	0.43	−2.23	0.59	−2.99	0.85	0.12	0.03	0.08	0.00	0.02	0.05
(N = 2)	Bottom ash	–	–	–	–	–	–	–	–	–	–	–	–	–	–
	Flue gas Hg^0	−0.60	0.10	−1.35	0.19	−2.09	0.31	−2.82	0.39	0.11	0.00	0.07	0.00	0.03	0.01
	Flue gas Hg^{2+}	−1.16	0.17	−1.48	0.20	−2.55	0.25	−3.01	0.36	−0.40	0.08	0.03	0.02	−0.28	0.03
	Flue gas Hg^P	−0.86	0.06	−1.43	0.17	−2.28	0.26	−2.94	0.33	−0.13	0.03	0.05	0.01	−0.07	0.01

*, No isotope data for bottom ash because of the low Hg content (<0.7 μg/kg).

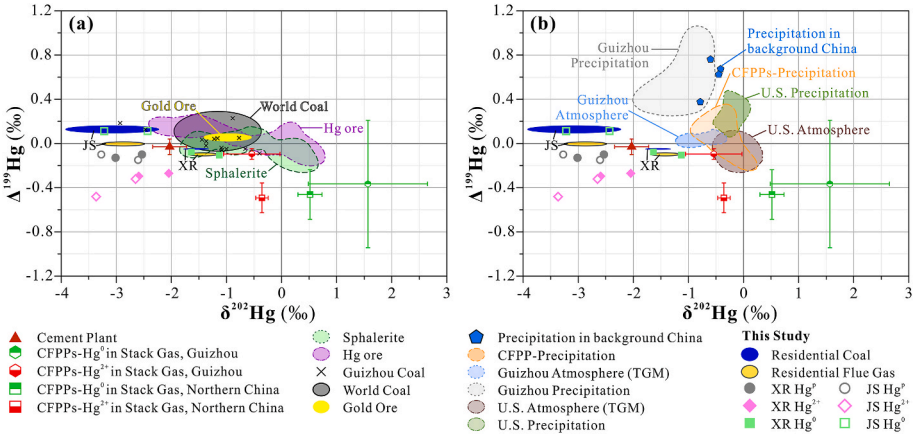

Fig. 4. Comparison of the Hg isotope composition of atmospheric emissions from the RCC with those in other important anthropogenic sources (a) and atmospheric samples (b).
Cement plant: On-site stack emissions (Li et al., 2021); CFPPs: on-site stack emissions in Guizhou (Guizhou Environmental Monitoring Center Station and Institute of Geochemistry, 2016), on-site stack emissions in northern China (Tang et al., 2017), precipitation around CFPPs (Huang et al., 2018); Sphalerite (Yin et al., 2016); Hg ores (Cooke et al., 2013; Feng et al., 2013; Stetson et al., 2009; Wiederhold et al., 2013; Yin et al., 2013); Guizhou coal (Biswas et al., 2008; Sun et al., 2014; Yin et al., 2014); World coal (Sun et al., 2016a); Gold ores (Smith, 2010); Guizhou atmosphere (TGM, Yu et al., 2016); Guizhou precipitation (Wang et al., 2015; Yuan et al., 2018); Precipitation in background China: Tibetan Plateau (Yuan et al., 2015).

the 2σ analytical uncertainty is 0.09‰ for Δ^{199}Hg. These results indicate that Hg isotopes in RCC are basically in balance.

3.5. MDF of Hg isotopes

Variations in δ^{202}Hg signals between feed coal and Hg^0 in flue gas are 0.21‰ and 0.17‰ for XR and JS, respectively, indicating that the Hg MDF is small during the combustion process in the residential stove. However, a negative shift of δ^{202}Hg from Hg^0 to Hg^{2+} in flue gas was observed, especially in XR (variation of 0.94‰, from −1.38‰ to −2.32‰), indicating that Hg MDF may have occurred during the oxidation process ($Hg^0 \rightarrow Hg^{2+}$), which resulted in Hg^{2+} being isotopically lighter than Hg^0. Similar to RCC, CFPPs also present lighter Hg^{2+} than Hg^0 in flue gas from the electrostatic precipitator outlet and wet flue gas desulfurization outlet ($\delta^{202}Hg^{2+}$ - $\delta^{202}Hg^0$ = −0.75‰ to −0.88‰) (Tang et al., 2017). The δ^{202}Hg value of Hg^P in XR (−2.77 ± 0.24‰) is lighter than those of Hg^0 (−1.38 ± 0.25‰) and Hg^{2+} (−2.32 ± 0.27‰), suggesting that Hg^P in the flue gas of XR is probably mainly absorbing Hg^{2+} in flue gas.

3.6. MIF of Hg isotopes

The Hg isotope MIF is generally caused by the nuclear volume effect (NVE) or magnetic isotope effect (MIE). NVE has been observed in liquid-vapor evaporation (Estrade et al., 2009; Ghosh et al., 2013), dark Hg^{2+} reduction (Zheng and Hintelmann, 2010), Hg^{2+}-thiol adsorption (Wiederhold et al., 2010), and atmospheric oxidation (Sun et al., 2016b), with $\Delta^{199}Hg/\Delta^{201}Hg$ ratios of 1.5–1.9. MIE has been observed during Hg photochemical reactions (such as Hg^{2+} photoreduction or methylmercury (MeHg) photodegradation), with $\Delta^{199}Hg/\Delta^{201}Hg$ ratios of 1.0–1.36 (Bergquist and Blum, 2007). In CFPPs, negative Δ^{199}Hg (−0.30‰ for Hg^0 and -0.46‰ for Hg^{2+}) with $\Delta^{199}Hg/\Delta^{201}Hg$ of ~1 was

observed in flue gas (mostly composed of Hg^0 and Hg^{2+}), which was believed to be inherited from fueled coal ($\Delta^{199}Hg = -0.34‰$) (Tang et al., 2017), and a $\Delta^{199}Hg/\Delta^{201}Hg$ of ~1 was observed for world coals (Sun et al., 2016a). However, in this study, the differences in Hg concentration and MIF between Hg^0 (1.35–9.26 μg/m^3, $\Delta^{199}Hg = -0.09‰$–0.11‰) and Hg^{2+} (0.34–0.37 μg/m^3, $\Delta^{199}Hg = -0.28‰$ to $-0.40‰$) in flue gas from residential stoves indicate that negative $\Delta^{199}Hg$ and $\Delta^{201}Hg$ of Hg^{2+} in the flue gas would not be inherited from the residential coals, but are related to the oxidation or transportation processes in the combustion chamber or smoke channel.

The chlorine (Cl) contents in coal from China and the world are 255 μg/g (N = 812) (Dai et al., 2012) and 180 μg/g (Ketris and Yudovich, 2009), respectively, and at these levels Cl in coal promotes Hg^0 oxidation in flue gas during some combustion processes, such as in CFIBs or CFPPs (Galbreath et al., 2005; Zhou et al., 2015). During coal combustion, Cl on the active sites directly oxidized Hg^0 into Hg_2Cl_2 or $HgCl_2$, which are then transferred from active sites into the gas phase (Wang et al., 2020b). Based on the results of Sun et al. (2016b), Hg^0–Cl oxidation resulted in a $\Delta^{199}Hg/\Delta^{201}Hg$ ratio of 1.88 ± 0.17, which is comparable with the $\Delta^{199}Hg/\Delta^{201}Hg$ of Hg^{2+} in the present study (1.76 ± 0.42), indicating that the negative MIF in Hg^{2+} is related to the oxidation of Cl in the RCC. This study highlights the difference in Hg transformation between RCC and CFPPs. The absence of significant Hg-MIF in boilers of CFPPs may be explained by the higher temperature (800–1400 °C) (Li et al., 2019b), which can reduce the NVE fractionation factor for Hg^0–$HgCl_2$ (Yang and Liu, 2015). Moreover, the high contents of oxidants (oxygen, bromine, metal oxides, etc.) in flue gas of CFPPs can accelerate the oxidation of Hg^0 (Galbreath et al., 2005; Yang and Pan, 2007; Zhang et al., 2016), resulting in limited extent of Hg-MIF as most of Hg^0 in flue gas of CFPPs is rapidly oxidized.

3.7. Implications

Without APCDs in RCC, the Hg atmospheric emission ratio (99.87 ± 0.09%) is very high compared to the other coal-dominated anthropogenic Hg emission sources, such as CFPPs in Guizhou, which have atmospheric emission ratios of less than 5% or even 1% (Guizhou Environmental Monitoring Center Station and Institute of Geochemistry, 2016; Li et al., 2019b; Tang et al., 2016). Based on Eq. (2), the emission factors (mg Hg/ton coal) of RCC are 112.15 mg Hg/ton coal and 30.33 mg Hg/ton coal for residential coal from XR and JS, respectively (Table S3). For Guizhou Province, the EF of the RCC source is 154.79 mg Hg/ton coal according to the weighted average (regional reserves) Hg content in Guizhou coal (155 μg/kg) (Li et al., 2013), which is approximately 5–160 times higher than the EF of 14 CFPPs in Guizhou (range: 0.94–32.98 μg Hg/kg coal; average 8.22 ± 10.48 μg Hg/kg coal) (Li et al., 2019b; Tang et al., 2016; Guizhou Environmental Monitoring Center Station and Institute of Geochemistry, 2016). Therefore, 951–1468 kg Hg is estimated to be emitted from RCC into the atmosphere annually in the past decade (Table S4) based on Eq. (3) and the coal consumption by RCC in Guizhou during 2007–2017 (Bureau of statistics of Guizhou Province, 2013, 2015, 2019).

RCC emissions have already caused some typical prevalent endemic diseases from exposure to arsenic (As), fluorine (F), and other potentially toxic trace elements (Finkelman and Centeno, 2020), indicating that RCC emissions have profound impacts on the regional atmospheric environment and human health. Tian et al. (2013) showed that RCC was the largest SO_2 contributor to some highly popularized areas in Guizhou Province in 2010, and contributed 50.7% of the total SO_2 emissions. Our on-site measurements also indicate that SO_2 emissions are one of concerning problems (Table S5). For Hg, Cui et al. (2019) estimated that the total Hg emissions from RCC in Guizhou were 48.9 tons between 1990 and 2016, with an annual Hg emission amount of 1.2–2.3 tons/yr, and serious atmospheric Hg contamination from uncontrolled coal burning has also been reported in other parts of China (Cao et al., 2021; Liang et al., 2014); especially in winter, more consumption of residential coal significantly increases atmospheric Hg concentrations compared with summer (Feng et al., 2003; Fu et al., 2011; Fu and Feng, 2015). In comparison, atmospheric Hg emissions from CFPPs in Guizhou Province are only ~0.5 tons/yr according to a recent on-site sampling study using OHM at 14 CFPPs (Guizhou Environmental Monitoring Center Station and Institute of Geochemistry, 2016; Tang et al., 2016). In summary, Hg emissions from RCC have great impacts on atmospheric Hg in Guizhou Province and even on the regional atmosphere because 85% of such emissions are in the form of Hg^0, which can be transported for long distances. Although prevalent endemic diseases caused by RCC have been alleviated in recent decades (Finkelman and Centeno, 2020), the impact of RCC on atmospheric Hg pollution deserves further study.

Using Eqs (4), (5), (8) and (9), the weighted average $\delta^{202}Hg$ and $\Delta^{199}Hg$ of total flue gas from the residential stove are estimated to be −1.47 ± 0.26‰ and −0.10 ± 0.01‰ for XR, and −3.00 ± 0.38‰ and 0.01 ± 0.02‰ for JS, respectively (Table S2). Significant differences in Hg isotope signatures were observed between atmospheric Hg emissions in XR and JS, but these values are consistent with the Hg isotope compositions of their coals (Fig. 3). Nevertheless, to reduce the uncertainty and obtain more accurate mean Hg isotope signatures from RCC in Guizhou, more field studies should be carried out. The Hg isotope compositions of important anthropogenic sources, including cement plant, CFPPs, sphalerite, Hg ore, coal, and gold ore, are illustrated in Fig. 4a. The $\delta^{202}Hg$ of Hg emissions from RCC (−2.23‰, averaged between cases of XR and JS) is comparable to that of cement plants (−2.03 ± 0.31‰) (Li et al., 2021) but is significantly lighter ($p < 0.05$) than those of stack emissions of CFPPs in Guizhou and other places in China (1.07 ± 0.95‰ for Hg^0, -0.44 ± 0.40‰ for Hg^{2+}, and −0.38 ± 0.38‰ for precipitation, Fig. 4b) (internal unpublished data; Huang et al., 2018; Tang et al., 2017), sphalerite (−0.47 ± 0.46‰, 1σ, N = 102) (Yin et al., 2016), Hg ore (−0.55 ± 0.52‰, 1σ, N = 70) (Cooke et al., 2013; Feng et al., 2013; Stetson et al., 2009; Wiederhold et al., 2013; Yin et al., 2013), and gold ore (−0.98 ± 0.44‰, P10–P90, N = 9) (Smith, 2010). The $\delta^{202}Hg$ values of total gaseous mercury (TGM) in atmospheric and total Hg in precipitation in Guizhou Province (Fig. 4b) are −0.61 ± 0.25‰ (1σ, N = 32) and −1.19 ± 0.79‰ (1σ, N = 25) (Yu et al., 2016; Wang et al., 2015; Yuan et al., 2018), respectively, which are significantly negative than those in the U.S. (0.10 ± 0.38‰ for TGM, 1σ, N = 7 and −0.33 ± 0.23‰ for precipitation, 1σ, N = 20, respectively (Gratz et al., 2010), and slightly negative than that of precipitation from background area in China (Tibetan Plateau, −0.56 ± 0.12‰, 2SD, N = 4) (Yuan et al., 2015). Values of $\delta^{202}Hg$ in the above-referenced atmospheric samples are more positive than those of atmospheric emissions from RCC in Guizhou (Fig. 4b) but are negative than those of CFPPs, sphalerite, Hg ore, and gold ore (Fig. 4a). These results indicate that RCC has a great negative-shifting impact on the $\delta^{202}Hg$ of atmospheric Hg. For MIF, $\Delta^{199}Hg$ of atmospheric Hg in Guizhou (0.04 ± 0.08‰, 2σ, N = 32) (Yu et al., 2016) and anthropogenic Hg sources (e.g., cement plants and RCC) (Li et al., 2021; this study) are all near zero, except for some CFPPs (−0.27 ± 0.22‰ for Hg^{2+}, −0.41 ± 0.44‰ for Hg^0) (internal unpublished data; Tang et al., 2017) and precipitation samples (0.53 ± 0.28‰ for Guizhou) (Yuan et al., 2018; Wang et al., 2015), and 0.30 ± 0.13‰ for U.S. (Gratz et al., 2010) because the redox chemistry process can cause significant MIF (Kwon et al., 2020; Tang et al., 2017; Gratz et al., 2010; Wang et al., 2015; Yuan et al., 2018). Cases with no significant MIF may be due to the lack of redox reactions because these samples are mainly composed of Hg^0 (Kwon et al., 2020).

Based on the Hg isotope compositions in residential coal, atmospheric Hg emissions from RCC can be effectively distinguished from other anthropogenic sources. It should be noted that atmospheric Hg emissions in earlier years from many large combustion units (such as CFPPs or CFIBs) without efficient APCDs should have isotope compositions similar to those from RCC emissions found in the present study; that is, Hg in coal is mostly emitted into the atmosphere, and $\delta^{202}Hg$ values are significantly negative than those of sphalerite, Hg ore, gold ore, and modern CFPPs (Fig. 4a). Such knowledge is of great significance

for retrieving historical Hg pollution data.

4. Conclusions

Atmospheric emission and isotope signatures of speciated Hg in RCC in rural areas of Guizhou Province, Southwest China were characterized by analyzing the Hg content and Hg isotope composition of onsite solid and flue gas samples. The total Hg concentration in flue gas is 1.80–9.65 μg/m^3, which is closely related to the Hg content in feed coal, and mainly in the form of Hg^0 (74.63–95.97%), followed by Hg^{2+} (3.54–20.44%), and with very low levels of Hg^p (0.49–4.93%). The amount of atmospheric Hg emissions from this source is estimated to be 1,468 kg in 2017 in the whole province. A weak shift of MDF (0.17‰–0.21‰ for δ^{202}Hg) and a near zero shift of MIF were found between feed coal and Hg^0 in flue gas. Significant Hg isotope shifts from Hg^0 to Hg^{2+} up to −0.94‰ and −0.51‰ for δ^{202}Hg and Δ^{199}Hg, respectively, were observed, which are probably related to oxidization by atomic chlorine. Hg emissions from RCC have a more negative δ^{202}Hg value than those of modern CFPPs and metal smelting; thus, this source sector has a negative-shifting impact on the isotope composition of atmospheric Hg.

CRediT authorship contribution statement

Xinyu Li: Methodology, Investigation, Software, Visualization, Writing - original draft. **Zhonggen Li:** Conceptualization, Funding acquisition, Methodology, Investigation, Supervision, Writing - review & editing. **Ji Chen:** Methodology, Investigation. **Leiming Zhang:** Funding acquisition, Writing - review & editing. **Runsheng Yin:** Writing - review & editing. **Guangyi Sun:** Methodology. **Bo Meng:** Methodology, Supervision. **Zikang Cui:** Methodology, Investigation. **Xinbin Feng:** Funding acquisition, Resources, Supervision.

Declaration of competing interest

The authors declare that they have no known competing financial interests or personal relationships that could have appeared to influence the work reported in this paper.

Acknowledgments

This work is financially supported by the Opening Fund of the State Key Laboratory of Environmental Geochemistry (SKLEG2020206), the Natural Science Foundation of China (U1612442 and 41967044), and K. C. Wong Education Foundation. Constructive comments from three anonymous reviewers are also greatly appreciated.

Appendix A. Supplementary data

Supplementary data to this article can be found online at https://doi.org/10.1016/j.atmosenv.2020.118175.

References

Adlane, B., Xu, Z., Xu, X., Liang, L., Han, J., Qiu, G., 2020. Evaluation of the potential risks of heavy metal contamination in rice paddy soils around an abandoned Hg mine area in Southwest China. Acta Geochim 39, 85–95.
AMAP/UNEP, 2008. Technical Background Report to the Global Atmospheric Mercury Assessment. Arctic Monitoring and Assessment Programme/UNEP Chemicals Branch, Nairobi.
Annals of China Coal-Volume of Guizhou Province, 1994. Coal Industry Press, Beijing (In Chinese).
Annals of Coal Industry of Guizhou Province, 1989. Guizhou People Press, Guiyang (In Chinese).
Bergquist, B.A., Blum, J.D., 2007. Mass-dependent and -independent fractionation of Hg isotopes by photoreduction in aquatic systems. Science 318, 417–420.
Biswas, A., Blum, J.D., Bergquist, B.A., Keeler, G.J., Xie, Z., 2008. Natural mercury isotope variation in coal deposits and organic soils. Environ. Sci. Technol. 42, 8303–8309.
Blum, J.D., Bergquist, B.A., 2007. Reporting of variations in the natural isotopic composition of mercury. Anal. Bioanal. Chem. 388, 353–359.
Blum, J.D., Sherman, L.S., Johnson, M.W., 2014. Mercury isotopes in earth and environmental sciences. Annu. Rev. Earth Planet Sci. 42, 249–269.
Bureau of Statistics of Guizhou Province, 2013. in Chinese). http://202.98.195.171:82/2013/indexch.htm. (Accessed 31 March 2020).
Bureau of Statistics of Guizhou Province, 2015. in Chinese). http://202.98.195.171:82/2015/zk/indexch.htm. (Accessed 31 March 2020).
Bureau of Statistics of Guizhou Province, 2019 (in Chinese)). http://202.98.195.171:82/2019/zk/indexch.htm. (Accessed 31 March 2020).
Cao, F., Meng, M., Shan, B., Sun, R., 2021. Source apportionment of mercury in surface soils near the Wuda coal fire area in Inner Mongolia, China. Chemosphere 263, 128348.
Cooke, C.A., Hintelmann, H., Ague, J.J., Burger, R., Biester, H., Sachs, J.P., Engstrom, D. R., 2013. Use and legacy of mercury in the Andes. Environ. Sci. Technol. 47, 4181–4188.
Cui, Z., Li, Z., Zhang, Y., Wang, X., Li, Q., Zhang, L., Feng, X., Li, X., Shang, L., Yao, Z., 2019. Atmospheric mercury emissions from residential coal combustion in Guizhou Province, Southwest China. Energy Fuels 33, 1937–1943.
Dai, S., Finkelman, R.B., 2017. Coal geology in China: an overview. Int. Geol. Rev. 60, 531–534.
Dai, S., Ren, D., Chou, C.L., Finkelman, R.B., Seredin, V.V., Zhou, Y., 2012. Geochemistry of trace elements in Chinese coals: a review of abundances, genetic types, impacts on human health, and industrial utilization. Int. J. Coal Geol. 94, 3–21.
Dai, S.F., Ren, D., Tang, Y.G., Yue, M., Hao, L.M., 2005. Concentration and distribution of elements in late permian coals from western Guizhou province, China. Int. J. Coal Geol. 61, 119–137.
Driscoll, C.T., Mason, R.P., Hing Man, C., Jacob, D.J., Nicola, P., 2013. Mercury as a global pollutant: sources, pathways, and effects. Environ. Sci. Technol. 47, 4967–4983.
Estrade, N., Carignan, J., Sonke, J.E., Donard, O.F.X., 2009. Mercury isotope fractionation during liquid–vapor evaporation experiments. Geochem. Cosmochim. Acta 73, 2693–2711.
Estrade, N., Carignan, J., Sonke, J.E., Donard, O.F.X., 2010. Measuring Hg isotopes in bio-geo-environmental reference materials. Geostand. Geoanal. Res. 34, 79–93.
Feng, X., Tang, S., Shang, L., Yan, H., Sommar, J., Lindqvist, O., 2003. Total gaseous mercury in the atmosphere of Guiyang, PR China. Sci. Total Environ. 304, 61–72.
Feng, X., Yin, R., Yu, B., Du, B., 2013. Mercury isotope variations in surface soils in different contaminated areas in Guizhou Province, China. Chin. Sci. Bull. 58, 249–255.
Finkelman, R.B., Centeno, J.A., 2020. Guizhou province, China: the birthplace of modern medical geology. Acta Geochi 39, 155–159.
Fu, X., Feng, X., 2015. Variations of atmospheric total gaseous mercury concentrations for the sampling campaigns of 2001/2002 and 2009/2010 and implications of changes in regional emissions of atmospheric mercury. Bull. China Soc. Mineral Petrol. Geochem. 334, 242–249 (In Chinese with English abstract).
Fu, X., Feng, X., Qiu, G., Shang, L., Zhang, H., 2011. Speciated atmospheric mercury and its potential source in Guiyang, China. Atmos. Environ. Times 45, 4205–4212.
Galbreath, K.C., Zygarlicke, C.J., Tibbetts, J.E., Schulz, R.L., Dunham, G.E., 2005. Effects of NOx, alpha-Fe_2O_3, gamma-Fe_2O_3, and HCl on mercury transformations in a 7-kW coal combustion system. Fuel Process. Technol. 86, 429–448.
Gao, W., Jiang, W., Zhou, M., 2019. The spatial and temporal characteristics of mercury emission from coal combustion in China during the year 2015. Atmos. Pollut. Res. 10, 776–783.
Ghosh, S., Schauble, E.A., Couloume, G.L., Blum, J.D., Bergquist, B.A., 2013. Estimation of nuclear volume dependent fractionation of mercury isotopes in equilibrium liquid-vapor evaporation experiments. Chem. Geol. 336, 5–12.
Gratz, L.E., Keeler, G.J., Blum, J.D., Sherman, L.S., 2010. Isotopic composition and fractionation of mercury in Great Lakes precipitation and ambient air. Environ. Sci. Technol. 44, 7764–7770.
Guizhou Environmental Monitoring Center Station (GEMCS), Institute of Geochemistry CAS (IGCAS), 2016. Study on the Characteristics of Atmospheric Mercury Emission from Coal-Fired Power Plants and Cement Plants in Guizhou Province (in Chinese).
Huang, S., Sun, L., Zhou, T., Yuan, D., Du, B., Sun, X., 2018. Natural stable isotopic compositions of mercury in aerosols and wet precipitations around a coal-fired power plant in Xiamen, southeast China. Atmos. Environ. 173, 72–80.
Ketris, M.P., Yudovich, Y.E., 2009. Estimations of Clarkes for Carbonaceous biolithes: world averages for trace element contents in black shales and coals. Int. J. Coal Geol. 78, 135–148.
Kwon, S.Y., Blum, J.D., Yin, R., Tsui, M.T.-K., Yang, Y.H., Choi, J.W., 2020. Mercury stable isotopes for monitoring the effectiveness of the Minamata Convention on Mercury. Earth Sci. Rev. 203, 103111.
Lefticariu, L., Blum, J.D., Gleason, J.D., 2011. Mercury isotopic evidence for multiple mercury sources in coal from the Illinois basin. Environ. Sci. Technol. 45, 1724–1729.
Li, X., Chen, J., Tang, L., Wu, T., Fu, C., Li, Z., Sun, G., Zhao, H., Zhang, L., Li, Q., Feng, X., 2021. Mercury isotope signatures of a pre-calciner cement plant in Southwest China. J. Hazard Mater. 401, 123384.
Li, X., Li, Z., Fu, C., Tang, L., Chen, J., Wu, T., Lin, C.J., Feng, X., Fu, X., 2019b. Fate of mercury in two CFB utility boilers with different fueled coals and air pollution control devices. Fuel 251, 651–659.
Li, Z., Chen, X., Liu, W., Li, T., Chen, J., Lin, C., Sun, G., Feng, X., 2019a. Evolution of four-decade atmospheric mercury release from a coal-fired power plant in North China. Atmos. Environ. 213, 526–533.
Li, Z., Feng, X., Li, G., Wang, X., 2013. Re-understanding of mercury concentrations of coal in Guizhou. In: 7th National Conference on Environmental Chemistry. Guiyang, China (In Chinese).

Li, Z., Li, X., Liu, J., Zhang, L., Chen, J., Feng, X., 2019c. Stone coal as a potential atmospheric mercury source in Da-Ba-Shan mountain areas, China. Int. J. Coal Geol. 206, 21–30.
Liang, Y., Liang, H., Zhu, S., 2014. Mercury emission from coal seam fire at Wuda, Inner Mongolia, China. Atmos. Environ. 83, 176–184.
Liu, K., Wu, Q., Wang, L., Wang, S., Liu, T., Ding, D., Tang, Y., Li, G., Tian, H., Duan, L., Wang, X., Fu, X., Feng, X., Hao, J., 2019. Measure-specific effectiveness of air pollution control on China's atmospheric mercury concentration and deposition during 2013-2017. Environ. Sci. Technol. 53, 8938–8946.
National Bureau of Statistic of China, 2019. in Chinese). http://www.stats.gov.cn/tjsj/ndsj/2019/indexch.htm. (Accessed 31 March 2020).
Scott, A.C., Glasspool, I.J., 2006. The diversification of Paleozoic fire systems and fluctuations in atmospheric oxygen concentration. Proc. Natl. Acad. Sci. U.S.A. 103, 10861–10865.
Smith, C.N., 2010. Isotopic Geochemistry of Mercury in Active and Fossil Hydrothermal Systems. University of Michigan. Doctor's thesis of.
Sonke, J.E., 2011. A global model of mass independent mercury stable isotope fractionation. Geochem. Cosmochim. Acta 75, 4577–4590.
Stetson, S.J., Gray, J.E., Wanty, R.B., Macalady, D.L., 2009. Isotopic variability of mercury in ore, mine-waste calcine, and leachates of mine-waste calcine from areas mined for mercury. Environ. Sci. Technol. 43, 7331–7336.
Streets, D.G., Hao, J., Wu, Y., Jiang, J., Chan, M., Tian, H., Feng, X., 2005. Anthropogenic mercury emissions in China. Atmos. Environ. 39, 7789–7806.
Streets, D.G., Devane, M.K., Lu, Z., Bond, T.C., Sunderland, E.M., Jacob, D.J., 2011. All-time releases of mercury to the atmosphere from human activities. Environ. Sci. Technol. 45, 10485–10491.
Sun, G., Sommar, J., Feng, X., Lin, C.J., Ge, M., Wang, W., Yin, R., Fu, X., Shang, L., 2016b. Mass-dependent and -independent fractionation of mercury isotope during gas-phase oxidation of elemental mercury vapor by atomic Cl and Br. Environ. Sci. Technol. 50, 9232–9241.
Sun, R., Enrico, M., Heimburger, L.E., Scott, C., Sonke, J.E., 2013. A double-stage tube furnace-acid-trapping protocol for the pre-concentration of mercury from solid samples for isotopic analysis. Anal. Bioanal. Chem. 405, 6771–6781.
Sun, R., Sonke, J.E., Heimbürger, L.E., Belkin, H.E., Liu, G., Shome, D., Cukrowska, E., Liousse, C., Pokrovsky, O.S., Streets, D.G., 2014. Mercury stable isotope signatures of world coal deposits and historical coal combustion emissions. Environ. Sci. Technol. 48, 7660–7668.
Sun, R., Sonke, J.E., Liu, G., 2016a. Biogeochemical controls on mercury stable isotope compositions of world coal deposits: a review. Earth Sci. Rev. 152, 1–13.
Tang, L., Liu, H., Feng, X., Li, Z., Fu, C., wang, H., Chen, J., Wang, S., 2016. Mercury emissions from a coal-fired power plant burning high ash content anthracite coal. Chin. J. Ecol. 35, 1351–1357 (In Chinese with English abstract).
Tang, S., Feng, C., Feng, X., Zhu, J., Sun, R., Fan, H., Wang, L., Li, R., Mao, T., Zhou, T., 2017. Stable isotope composition of mercury forms in flue gases from a typical coal-fired power plant, Inner Mongolia, northern China. J. Hazard Mater. 328, 90–97.
Tian, H., Qiu, P., Cheng, K., Gao, J., Lu, L., Liu, K., Liu, X., 2013. Current status and future trends of SO2 and NOx pollution during the 12th FYP period in Guiyang city of China. Atmos. Environ. 69, 273–280.
Tian, H.Z., Wang, Y., Xue, Z.G., Cheng, K., Qu, Y.P., Chai, F.H., Hao, J.M., 2010. Trend and characteristics of atmospheric emissions of Hg, As, and Se from coal combustion in China, 1980-2007. Atmos. Chem. Phys. 10, 11905–11919.
Tong, Y., Yue, T., Gao, J., Wang, K., Wang, C., Zuo, P., Zhang, X., Tong, L., Liang, Q., 2020. Partitioning and emission characteristics of Hg, Cr, Pb, and as among air pollution control devices in Chinese coal-fired industrial boilers. Energy Fuels 34, 7067–7075.
Wang, F., Li, G., Wang, S., Wu, Q., Zhang, L., 2020b. Modeling the heterogeneous oxidation of elemental mercury by chlorine in flue gas. Fuel 262, 116506.
Wang, Q., Shen, W., Ma, Z., 2000. Estimation of mercury emission from coal combustion in China. Environ. Sci. Technol. 34, 2711–2713.
Wang, X., Lin, C.J., Feng, X., Yuan, W., Fu, X., Zhang, H., Wu, Q., Wang, S., 2018. Assessment of regional mercury deposition and emission outflow in Mainland China. J. Geophys. Res. Atmos. 123, 9868–9890.
Wang, X., Yuan, W., Lin, C.J., Luo, J., Wang, F., Feng, X., Fu, X., Liu, C., 2020a. Underestimated sink of atmospheric mercury in a deglaciated forest chronosequence. Environ. Sci. Technol. 54, 8083–8093.
Wang, Z., Chen, J., Feng, X., Hintelmann, H., Yuan, S., Cai, H., Qiang, H., Wang, S., Wang, F., 2015. Mass-dependent and mass-independent fractionation of mercury isotopes in precipitation from Guiyang, SW China. Comptes. Rendus. 347, 358–367.
Wiederhold, J.G., Cramer, C.J., Daniel, K., Infante, I., Bourdon, B., Kretzschmar, R., 2010. Equilibrium mercury isotope fractionation between dissolved Hg(II) species and thiol-bound Hg. Environ. Sci. Technol. 44, 4191–4197.
Wiederhold, J.G., Smith, R.S., Siebner, H., Jew, A.D., Brown Jr., G.E., Bourdon, B., Kretzschmar, R., 2013. Mercury isotope signatures as tracers for Hg cycling at the New Idria Hg Mine. Environ. Sci. Technol. 47, 6137–6145.
Wu, Q., Wang, S., Li, G., Liang, S., Lin, C.J., Wang, Y., Cai, S., Liu, K., Hao, J., 2016. Temporal trend and spatial distribution of speciated atmospheric mercury emissions in China during 1978–2014. Environ. Sci. Technol. 50, 13428–13435.
Yang, H., Pan, W., 2007. Transformation of mercury speciation through the SCR system in power plants. J. Environ. Sci. 19, 181–184.
Yang, S., Liu, Y., 2015. Nuclear volume effects in equilibrium stable isotope fractionations of mercury, thallium and lead. Sci. Rep. 5, 1–12.
Yin, R., Feng, X., Hurley, J.P., Krabbenhoft, D.P., Lepak, R.F., Hu, R., Zhang, Q., Li, Z., Bi, X., 2016. Mercury isotopes as proxies to identify sources and environmental impacts of mercury in sphalerites. Sci. Rep. 6, 1–8.
Yin, R., Feng, X., Chen, J., 2014. Mercury stable isotopic compositions in coals from major coal producing fields in China and their geochemical and environmental implications. Environ. Sci. Technol. 48, 5565–5574.
Yin, R., Feng, X., Wang, J., Li, P., Liu, J., Zhang, Y., Chen, J., Zheng, L., Hu, T., 2013. Mercury speciation and mercury isotope fractionation during ore roasting process and their implication to source identification of downstream sediment in the Wanshan mercury mining area, SW China. Chem. Geol. 336, 72–79.
Yin, R.S., Feng, X.B., Foucher, D., Shi, W.F., Zhao, Z.Q., Wang, J., 2010. High precision determination of mercury isotope ratios using online mercury vapor generation system coupled with multicollector inductively coupled plasma-mass spectrometer. Chin. J. Anal. Chem. 38, 929–934.
Yu, B., Fu, X., Yin, R., Zhang, H., Wang, X., Lin, C.J., Wu, C., Zhang, Y., He, N., Fu, P., Wang, Z., Shang, L., Sommar, J., Sonke, J.E., Maurice, L., Guinot, B., Feng, X., 2016. Isotopic composition of atmospheric mercury in China: new evidence for sources and transformation processes in air and in vegetation. Environ. Sci. Technol. 50, 9262–9269.
Yuan, S., Chen, J., Cai, H., Yuan, W., Wang, Z., Huang, Q., Liu, Y., Wu, X., 2018. Sequential samples reveal significant variation of mercury isotope ratios during single rainfall events. Sci. Total Environ. 624, 133–144.
Yuan, S.L., Zhang, Y., Chen, J.B., Kang, S.C., Qiang, H., 2015. Large variation of mercury isotope composition during a single precipitation event at Lhasa City, Tibetan Plateau, China. Procedia Earth Planet. Sci. 13, 282–286.
Yudovich, Y.E., Ketris, M.P., 2005. Mercury in coal: a review Part 2. Coal use and environmental problems. Int. J. Coal Geol. 62, 135–165.
Zhang, L., Wang, S., Wang, L., Wu, Y., Duan, L., Wu, Q., Wang, F., Yang, M., Yang, H., Hao, J., Liu, X., 2015. Updated emission inventories for speciated atmospheric mercury from anthropogenic sources in China. Environ. Sci. Technol. 49 (5), 3185–3194.
Zhang, L., Wang, S., Wu, Q., Wang, F., Lin, C.J., Zhang, L., Hui, M., Yang, M., Su, H., Hao, J., 2016. Mercury transformation and speciation in flue gases from anthropogenic emission sources: a critical review. Atmos. Chem. Phys. 16, 2417–2433.
Zhang, Q., Jiang, P., Qu, L., Huang, W., 2019. Mercury emission and pollution from the decentralized coal combustion in a typical rural area of Guizhou Province. Earth Environ. 47, 637–643 (In Chinese with English Abstract).
Zhao, Y., Zhong, H., Zhang, J., Nielsen, C.P., 2015. Evaluating the effects of China's pollution controls on inter-annual trends and uncertainties of atmospheric mercury emissions. Atmos. Chem. Phys. 15, 4317–4337.
Zheng, B., Zhang, J., Ding, Z., Yu, X., Zhou, D., Mao, D., Su, H., 1999. Issues of health and disease relating to coal use in southwestern China. Int. J. Coal Geol. 40, 119–132.
Zheng, L., Sun, R., Hintelmann, H., Zhu, J., Wang, R., Sonke, J.E., 2018. Mercury stable isotope compositions in magmatic-affected coal deposits: new insights to mercury sources, migration and enrichment. Chem. Geol. 479, 86–101.
Zheng, W., Hintelmann, H., 2010. Nuclear field shift effect in isotope fractionation of mercury during abiotic reduction in the absence of light. J. Phys. Chem. 114, 4238–4245.
Zheng, X., Dai, S., Nechaev, V., Sun, R., 2020. Environmental perturbations during the latest Permian: evidence from organic carbon and mercury isotopes of a coal-bearing section in Yunnan Province, southwestern China. Chem. Geol. 549, 119680.
Zhou, Z.J., Liu, X.W., Zhao, B., Chen, Z.G., Shao, H.Z., Wang, L.L., Xu, M.H., 2015. Effects of existing energy saving and air pollution control devices on mercury removal in coal-fired power plants. Fuel Process. Technol. 131, 99–108.